Meteoritics & Planetary Science 41, Nr 8, 1163–1173 (2006)
Abstract available online at http://meteoritics.org

Polygonal impact craters in the Argyre region, Mars: Evidence for influence of target structure on the final crater morphology

T. ÖHMAN[1, 2*], M. AITTOLA[2], V.-P. KOSTAMA[2], M. HYVÄRINEN[2], and J. RAITALA[2]

[1]Department of Geosciences, Division of Geology, P.O. Box 3000, FI-90014 University of Oulu, Oulu, Finland
[2]Department of Physical Sciences, Division of Astronomy, P.O. Box 3000, FI-90014 University of Oulu, Oulu, Finland
*Corresponding author. E-mail: teemu.ohman@oulu.fi

(Received 16 November 2005; revision accepted 26 April 2006)

Abstract–Impact craters that in plan view are distinctly polygonal rather than circular or elliptical are common on Mars and other planets (Öhman et al. 2005). Their actual formation mechanism, however, is somewhat debatable. We studied the polygonal craters of different degradational stages in the region of the Argyre impact basin, Mars. The results show that in the same areas, heavily degraded, moderately degraded, and fresh polygonal craters display statistically similar strike distributions of the straight rim segments. The fact that the strike distributions are not dependent on lighting conditions was verified by using two data sets (Viking and MOC-WA) having different illumination geometries but similar resolutions. In addition, there are no significant differences in the amount of polygonality of craters in different degradational stages. These results clearly imply that large-scale polygonality is not caused by degradation, but originates from the cratering process itself, concurring with the findings regarding lunar craters by Eppler et al. (1983). The straight rims of polygonal craters apparently reflect areal fracture patterns that prevail for a geologically long time.

BACKGROUND AND THE PURPOSE OF THE STUDY

This project was initiated in order to 1) better constrain the origin of planimetric polygonality of impact craters (see Öhman et al. 2005 for a discussion) and thus understand the effects of preexisting structures of the target material during the formation of impact craters (this work). Another, future objective is to 2) find out how polygonal impact craters (PICs) reflect the complex geotectonic history of the Argyre impact basin's surroundings, and how the structural data obtained from PICs in the Argyre region match findings from other basins (Hellas and Isidis; Öhman et al. 2005) or from other tectonic indicators (e.g., graben and ridges; Öhman et al., Forthcoming).

Regarding the formation mechanisms of polygonal craters, we adhere to the hypotheses formulated by Shoemaker (1963) and Roddy (1978), and especially Eppler et al. (1983). According to these authors, polygonal outline of simple craters forms in the excavation stage, when the excavation flow expands more rapidly along preexisting fractures, resulting in straight rim segments bisecting the fracture trends. The best, and to our knowledge the only, well-documented field evidence for this formation model comes from the Barringer crater, where the target rocks have two dominating regional joint directions perpendicular to each other (Shoemaker 1963; Roddy 1978). These joint set directions form diagonals across the roughly square-shaped crater. Thus, the joint sets make an angle of about 45° with respect to the straight rim segments. However, impact and explosion experiments in fractured targets (Fulmer and Roberts 1963; Gault et al. 1968) have indicated that two dominating orthogonal fracture directions don't necessarily lead to squarish craters, but also other shapes, and rim orientations with respect to fracture directions may occur.

In complex craters, the formation scenario is supposedly somewhat different. The unstable crater rim collapses along fractures in the modification stage and thus the straight rims parallel the preexisting fracture directions (Eppler et al. 1983; Schultz 1976). The best terrestrial example of a polygonal complex crater is the Söderfjärden structure in western Finland. The target rocks in Söderfjärden have two regional orthogonal fracture directions (Abels 2003; Talvitie et al. 1975; Raitala 1985). The third dominating structural trend comes from the metamorphic fabric bisecting the fracture trends roughly in an angle of 45° (Raitala 1985; Abels 2003). All three directions can readily be seen in the present-day topographic appearance of this notably hexagonal impact structure, as well as in its geophysical signature (Abels 2003). It is worth noting that a hexagonal shape is also quite typical for polygonal impact craters on the Moon (e.g.,

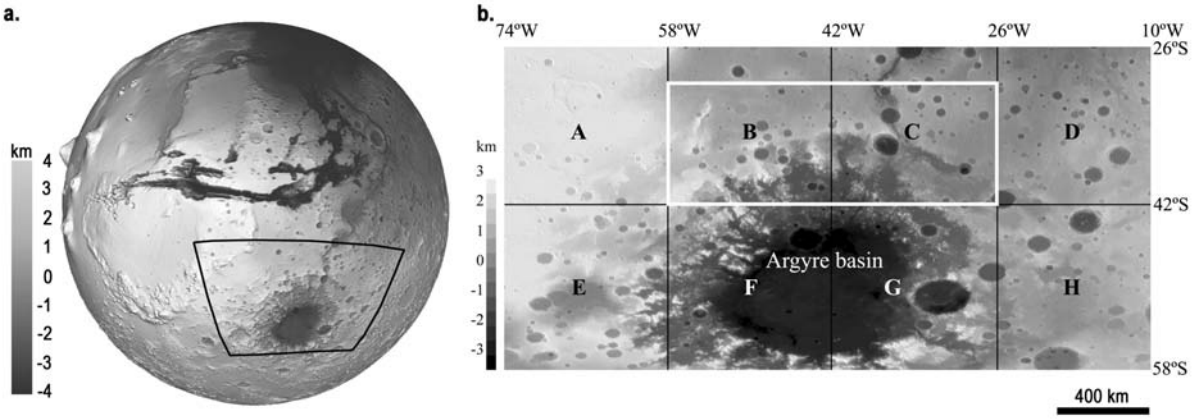

Fig. 1. Mars Orbiter Laser Altimeter topography of the study area. In (a) the hemispherical projection, with a ten-fold vertical exaggeration, the black trapezoid delineates the study area shown with more detail in (b). Note the Tharsis bulge in the western horizon and Valles Marineris north and northwest from the Argyre basin. In (b), the block division (A–H) used in this work is shown. The white box denotes the area that was studied using both Viking and MOC-WA mosaics. In (b), the scale bar holds true only around 40°S due to map projection used.

Baldwin 1963; Kopal 1966) and on Mars (Öhman et al. 2005).

Sometimes differential erosion has been invoked as a means to explain the polygonal outline of some terrestrial impact structures, including proven but also "probable" impact structures (Rossi et al. 2003; discussed by Abels 2003 and also briefly mentioned by Laurén et al. 1978). Although this may be true in some cases, it is worth noting that Eppler et al. (1983) already demonstrated the negligible role of degradation in the large-scale polygonality of lunar impact craters. By analogy, this should hold for craters on other planetary bodies as well. In this work, we study whether or not degradation of craters (see, e.g., Grant and Schultz 1993) can be attributed to the formation of polygonal impact craters within the region of the Argyre impact basin in the southern hemisphere of Mars.

GEOLOGIC OUTLINE OF THE ARGYRE REGION

Our study area (10°–74°W, 26°–58°S) (Fig. 1) covers a large area surrounding the Early Noachian Argyre impact basin. The Argyre basin with diameter of over 1500 km (Tanaka et al. 1992) is located in the southern highlands of Mars, southeast of the Tharsis rise and south to southeast of Valles Marineris. In the west, our study area reaches Aonia Terra, and in the east it extends to the western part of Noachis Terra, the type region of heavily cratered Noachian highlands. In contrast, the northwestern part of our study area partly covers the Hesperian volcanic plains (Scott and Tanaka 1986) of Thaumasia Planum. The central part of the study area is largely covered by sparsely cratered Argyre Planitia, which has a complex geologic history with several geological processes—mainly glacial and fluvial/lacustrine—contributing to its current appearance (Hiesinger and Head 2002).

Overall, Argyre has a pristine appearance compared to the other large impact basins on Mars (Hellas and Isidis), although it is not significantly younger (e.g., Hiesinger and Head 2002). In contrast to Isidis and Hellas, the Moho is deeper in Argyre (Neumann et al. 2004). The Argyre impact excavated a relatively thick crust, the minimum crustal thickness being 23.7 km, compared to only 5.8 km and 6.6 km in Isidis and Hellas basins, respectively. In Argyre, the excavation of the crust is also concentrated only to the center of the basin: the crust's thickness increases rapidly at distances more than 350 km from the center (Neumann et al. 2004). The thicker crust and deep Moho may be related to the more pristine appearance of the Argyre basin.

The magnetic anomalies, especially in the southern part of the Argyre region, are patchy and generally weak, thus giving no clear-cut indication of the possible early Martian plate tectonics that have been hypothesized based on the strong, linear, east-west-trending magnetic anomalies so vivid in Terra Cimmeria and Terra Cirenum (e.g., Acuña et al. 1999; Connerney et al. 1999; Purucker et al. 2000). However, in the northern part of our study area, the most recent data (Connerney et al. 2005) show slightly stronger linear magnetic anomalies trending ESE (parallel to Valles Marineris) and SE.

The fact that impact basins tend to create radial and concentric tectonic patterns around them is well known, also with respect to Mars (e.g., Schultz et al. 1982; Wichman and Schultz 1989; Öhman et al. 2005). Such tectonic structures can be seen in the Argyre region as well. Hodges (1980), in her geologic map of the Argyre quadrangle, noted, e.g., narrow concentric troughs, especially in the northwest. In their study of the tectonics of the Argyre basin, Thomas and Masson (1984) observed many concentric but discontinuous scarps. They also measured lineaments in the northwestern half of their "Nereidum Formation" (approximately

corresponding to the unit called "Argyre basin rim material" by Hodges 1980) and found a dominance of lineaments tangential and especially radial to the basin. In addition, Thomas and Masson (1984) found an indication of an important tectonic lineation trending 020°–050° that is older than the Argyre impact. They concluded that the Argyre basin has no tectonic influence beyond what they call an "outer scarp" (apparently about 1150 km from the basin center?).

The research carried out by Chicarro et al. (1985) focused on various types of ridges throughout the whole planet. Their high- and low-relief ridges have a general NNW-NNE trend in the Argyre region. Ridges in old cratered plains display a northerly strike, while ridges in younger plains trend a bit more towards NNE-NE. When a basin-concentric component of their data is omitted, a NNW-striking ridge orientation emerges. When directions of all ridge types (except of course ridge rings that most likely are buried impact craters) of Chicarro et al. (1985) are summed up, it appears that areas west from the basin are dominated by NE-striking ridges, while ridges in the eastern and northeastern surroundings of the basin are striking NNW. North from the basin a broader, generally northerly ridge strike is apparent (Chicarro et al. 1985).

Schultz (1985) investigated scarps, graben, and channel-wall scarps in sections of the Argyre and Margaritifer Sinus regions that partly reach our study area. In the Argyre area, Schultz had a very low number of measurements, but there appears to be a maxima in scarps trending N-NNE, and in graben trending E-ENE. In Margaritifer Sinus, scarps and channel-wall scarps that strike NNE are dominating, with a smaller scarp maxima in ESE-strike that matches the main strike of the graben. On the geologic map by Scott and Tanaka (1986), the ESE trend of graben is apparent as well, in addition to ridges trending N-NNE. These NNE and ESE strikes of ridges and graben, respectively, perfectly match our own preliminary studies from the northwestern part of our study area (Öhman et al. 2006).

In general, the tectonics of the study area are controlled by the Argyre impact and the resulting basin-radial and basin-concentric structures, with a significant overprint by the Tharsis bulge. The ridges are usually concentric to Tharsis and faults are radial (Scott and Tanaka 1986), although in highly cratered terrains, features radial to Tharsis are mostly lacking (Schultz 1985). Another dominating tectonic structure are the graben, especially north from the basin, trending roughly east or east-southeast. A more comprehensive comparative study on the tectonic directions revealed by ridges, graben, channels, and polygonal craters and their implications to the geologic history of the Argyre region is in progress.

METHODS AND RATIONALE

The primary data set used was NASA's Viking Orbiter MDIM 2.0 (Mars mosaicked digital image model) global photomosaic with a resolution of 231.4 m/pixel at the equator (Kirk et al. 2000). MDIM 2.0 in conformal Mercator projection was produced by the U.S. Geological Survey and obtained from NASA's Planetary Data System. However, to account for a possible bias caused by Viking's illumination geometry (see below), a smaller set of PICs were studied also from NASA's Mars Global Surveyor's Mars Orbiter Camera Wide Angle (MOC-WA) image mosaics with a similar resolution (231.5 m/pixel). The MOC-WA images were obtained from Malin Space Science Systems and then reprojected from simple cylindrical to Mercator projection. The illumination geometry in the MOC-WA images is in a broad sense fairly uniform, whereas it varies greatly in the Viking mosaic. Despite this, the Viking data set is much better than MOC-WA for this kind of study due to its lower incidence angle, which makes the detection of topographic features like crater rims easier.

It is a well-known (e.g., Schultz 1976) problem in photogeology that the direction of illumination in the image may significantly alter the appearance of various features on a planetary surface by enhancing some structures, while other structures (even prominent ones) may almost disappear. The direction of illumination can slightly affect even the apparent strikes of lineaments, and polygonal crater rims are of course no objection to this rule. The effect of illumination geometry —whether or not it is statistically important—was taken into account by studying a smaller area north from the Argyre basin (30°S–42°S, 26°W–58°W) (Fig. 1) using both Viking and MOC-WA images. MOC-WA mosaic was investigated independently from Viking imagery. For rim strike measurements, however, only the craters that had been identified as polygonal in both data sets were included. If there were a major difference in the overall distribution of the strikes of polygonal crater rim segments caused by lighting conditions, it should become evident by comparing the two data sets, since they have notably different illumination geometries.

Based on thorough visual inspection of images, we applied a fairly strict yet subjective definition for a polygonal crater: to be classified as a polygonal impact crater, the structure had to have at least two straight rim segments, the strikes of which were measured, with a notable angle between them (see Fig. 2; the definition is the same as in Öhman et al. 2005). In addition, the classification had to be agreed on by two researchers.

Occasionally, it is possible that the outline of a crater can become somewhat polygonal because, e.g., fluvial, volcanic, or mass-wasting processes may cover or erode some section of the crater rim. A much more common scenario is when another, younger impact distorts the crater's rim so it becomes in a broad sense "polygonal" (Fig. 3). As such "polygonal" craters are not truly polygonal in the sense that we use the term, they were discarded from the study. Note also that we refer to the large-scale polygonality of craters, so the smaller-scale irregular scalloping (e.g., Schultz 1976) of crater walls, which is typical for complex craters, is not an issue here.

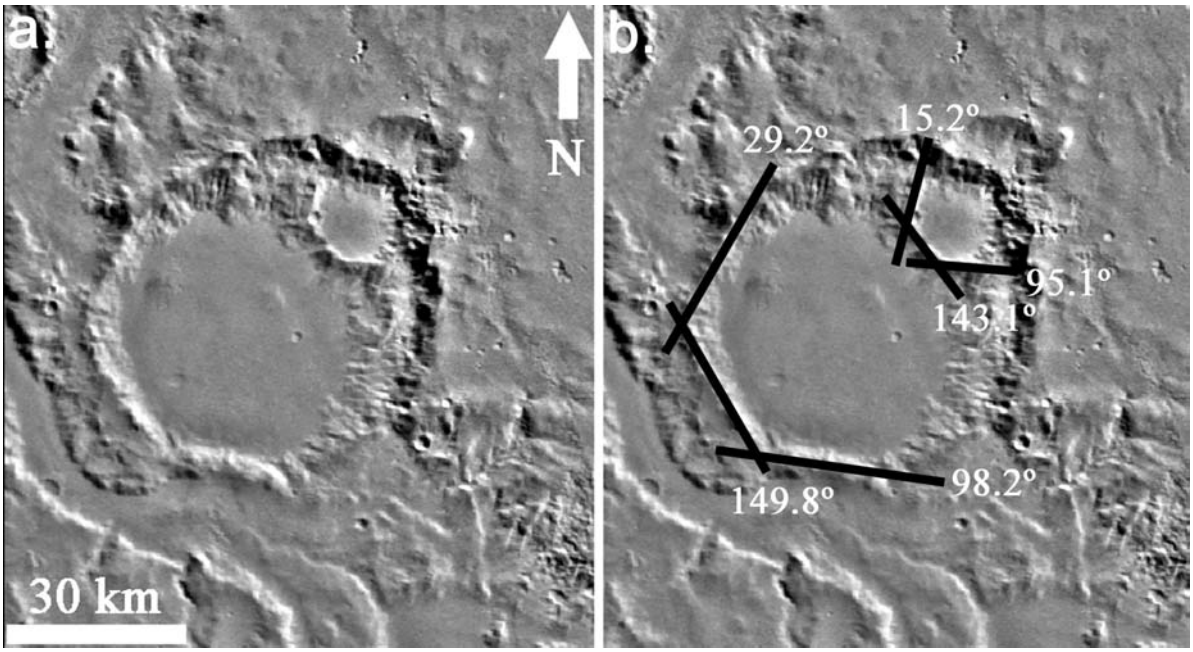

Fig. 2. An example of polygonal impact craters (PICs) (a) north of the Argyre basin (36.3°W, 30.5°S), with the interpretation and measurement of straight rim segments (b). Note that the smaller crater's rims parallel those of the larger one's, despite the fact that the larger crater's impact should have destroyed any preexisting fracture patterns. A possible explanation is that the regional fracture pattern is quite deep-seated and has been reactivated after the formation of the larger crater, thus affecting also the shallower depths and therefore the formation of the smaller crater.

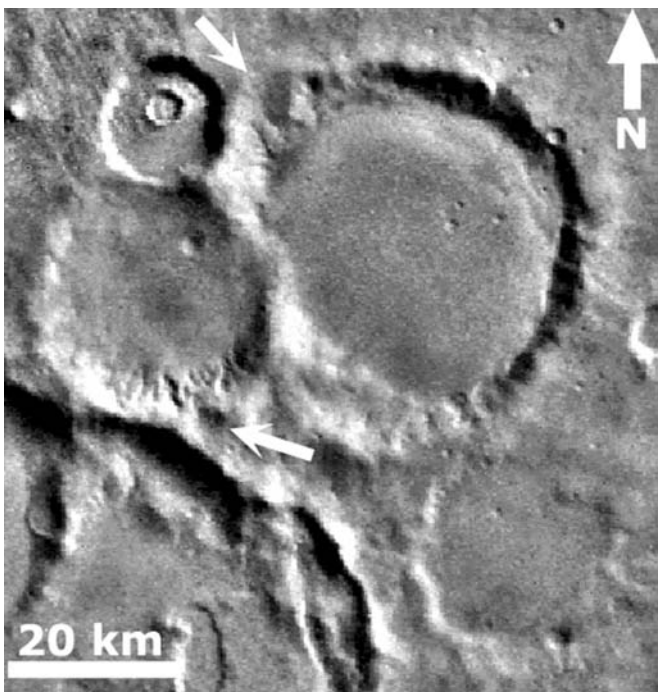

Fig. 3. Partly superposed craters west of the Argyre basin (63.3°W, 42.8°S) that display a noncircular and in one sense a "polygonal" outline, but are not considered as polygonal impact craters in this study. The largest crater (named THU Br) is "polygonal" mainly due to partial superposition of the smaller craters on its western side, which themselves are also partly "polygonal" due to the overlapping of the rims. In addition, small channels (white arrows) have backwasted the rims in places, thus increasing the craters' irregularity. Although there are some straight segments in the eastern rim of the crater THU Br, that is not enough to make it a true polygonal impact crater. Note also the irregular shallow depression—probably a very highly degraded and modified impact crater—with some rather straight segments in the lower right corner of the image. None of the depressions in the figure are regarded as polygonal impact craters. Compare with craters in Figs. 2 and 6.

The degradational stage of each polygonal crater was estimated, using MDIM 2.0 mosaic, by classifying them into three easily distinguishable groups: craters with a rim and a preserved ejecta blanket (henceforth called "fresh"), craters with no ejecta but a clearly discernible rim ("rimmed"), and craters with very heavily or completely degraded rim ("degraded"). This classification clearly is not even, since the group of "rimmed" craters generally outnumbers the other groups. This does create some problems with statistics, but the ease and unambiguity of such classification outweigh the slight difficulties in statistical investigation. A larger amount of degradational classes would make statistical analysis unreliable due to the small number of strike measurements in each class.

For practical reasons (file sizes, etc.), the study area was divided into eight "blocks" (see Fig. 1). As these blocks are arbitrary, each block contains craters formed in target materials of different origins and ages. However, this affects mainly the geologic and tectonic interpretation of the Argyre region using PICs, ridges, graben, and channels, which will be reported separately (Öhman et al. 2006; Öhman et al., Forthcoming). A more rational areal division, e.g., based on geologic units or azimuthal direction with respect to the basin, can be applied when desired. For the present study, the block division can be regarded as adequate.

The precision of the measurement of the strikes of straight rim segments is about ±5°, and often better. The strike measurements from each block were plotted in histograms with 10° class intervals, each of the degradational stages separately. 15° and 20° class intervals were also tested, but these didn't affect our major results and conclusions.

The similarity, or dissimilarity, of the strike distributions was studied by two-tailed Kolmogorov-Smirnov (K-S) two-sample test, which tells us whether or not two sample distributions are drawn from the same population. The K-S test has several advantages compared to the more familiar chi-square test. The most important strong points of the K-S test are that it can be used reliably with smaller sample sizes than the chi-square test, and that the number of measurements in the samples can be highly variable without complicating the calculation procedure. The critical values (in 95% confidence level) for the K-S test were taken from Davis (2002), and for larger numbers of measurements ($n_1 + n_2 > 100$) the approximate critical values were calculated with the formula given by Cheeney (1983). In the few cases where the chi-square test was applicable, it was also used for verification.

In the context of our study, the K-S statistic enables us to determine whether degradation acting at random is the cause of the polygonal shape, or if the shape's origin lies in the properties of the target material and in the cratering process itself. In other words, fresh and heavily degraded craters are unlikely to have similar strike distributions if degradation is causing the polygonality, but if dominant fracture directions that have remained the same for a long time affect the shape of the crater, then one would expect fresh and degraded polygonal craters to have somewhat similar rim strike distributions.

RESULTS

Altogether, 269 polygonal impact craters in the Argyre region were studied, each classified according to their degradational state and number of straight rim segments. The majority of the polygonal craters were complex craters, typical well-defined examples having a diameter of about 10–35 km (on Mars the simple-to-complex transition takes place in about 5–7 km diameter range) (e.g., Pike 1980; Garvin et al. 2003). The interior morphologies of the PICs reflect the typical crater diversity on Mars, i.e., some had "ordinary" central peaks or merely flat floors while others displayed central pits. Ejecta blankets also varied greatly from layered to radial ejecta morphologies (Barlow et al. 2000). A more detailed tectonic study also involving analysis on the diameter, interior, and ejecta morphologies of the PICs in the Argyre region will be reported in a companion paper (Öhman et al., Forthcoming).

At these 269 craters, we measured 820 straight rim segment strikes. Figures 4 and 5 exemplify the main results of this work. Figure 4 depicts the percentages of PICs of different degradational stages classified by their amount of polygonality as measured by the number of straight rim segments. In a broad sense, the distribution patterns are strikingly similar in all classes of polygonality. Rimmed craters are by far the most common type—with a share of >50% in each polygonality class—followed by degraded and fresh craters having roughly equal percentages. This is naturally due to the fact that the rimmed craters are, in general, so prominent among all impact craters on Mars compared to other degradational classes used in this study. It is worth noting that degraded craters are not more common in the class of most polygonal craters (5–6 straight sides) than in the least polygonal (2 straight sides). Therefore, degradational stage of the craters is apparently not reflected in their large-scale polygonality.

Figure 5 shows the percentages of rim strikes in 15° bins in degraded, rimmed, and fresh polygonal craters in area D northeast from the Argyre basin. Although the diagrams have some small discrepancies, the overall shape of the plots is very similar. Using 10° bins doesn't change this fact. The similarity was also confirmed by a statistical approach: according to the K-S statistic in the 95% confidence level, the samples are drawn from the same population. For this area, the chi-square test was also used (with 15° bins), and it confirmed the result of the K-S test. In practice, the result indicates that the dominating directions displayed by the straight rim segment strikes of PICs are the same for degraded (71 measurements), rimmed (67 measurements), and fresh (29 measurements) craters.

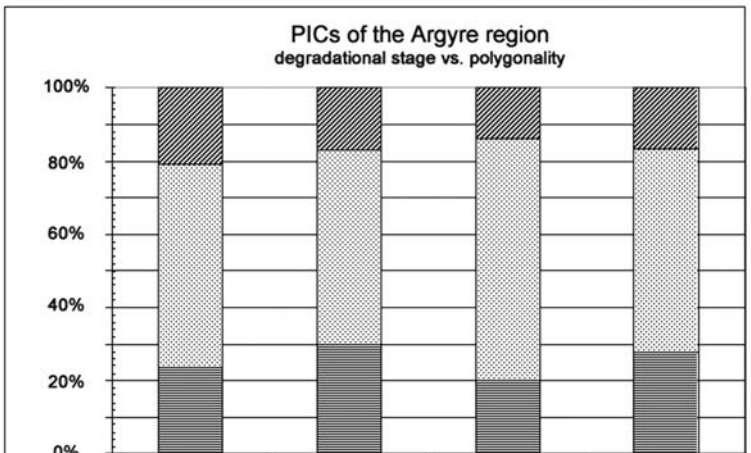

	2 straight sides	3 straight sides	4 straight sides	5-6 straight sides
fresh	16	21	7	3
rimmed	43	66	33	10
degraded	18	37	10	5
total n	77	124	50	18

Fig. 4. The percentages of fresh, rimmed, and degraded PICs are roughly equal in all polygonality classes, classified here by the number of straight rim segments. Note the significant differences in the number of measurements between different classes.

The above holds for other areas as well. Using the arbitrary block division, we checked six blocks (blocks F and G, which include the interior of the Argyre basin, are disregarded here due to the low number of measurements) and compared the strike distributions of each degradational class with each other (i.e., degraded/rimmed, degraded/fresh, and rimmed/fresh). All blocks were tested with both 10° and 15° divisions, with congruent results (Table 1). Thus, we made 36 different comparisons utilizing the K-S test in the 95% confidence level. Using 10° bins, five comparisons showed that the two rim strike distributions were not drawn from the same population. With 15° divisions, significant discrepancies appeared in three comparisons. The discrepancies typically appeared in areas with a rather low number of measurements in one of the degradational classes, and usually involved fresh craters, which are the rarest degradational class in our study (except in block A, where degraded craters are a rarity). Thus, we assume that with a larger number of measurements, discrepancies would have been even smaller. This is supported by the fact that out of eight comparisons that didn't fulfill the K-S test in the 95% confidence level, five were extremely close (the difference from the critical value being about 0.01).

The comparison between Viking and MOC-WA images showed, as was to be expected, that there are major differences in the subjectively determined polygonality of individual impact craters when correlating images with different illumination geometries (Fig. 6). A crater that appears rather circular in a MOC-WA image may look distinctly polygonal in a Viking image, and vice-versa. In general, it is easier to see polygonality in Viking imagery because of the lower incidence angle that enhances the appearance of topographic variations. The spatial distribution of polygonal craters looks somewhat different depending on the data set used. However, when we study those craters that have been independently classified as polygonal in both Viking and MOC-WA data sets, an interesting fact emerges. Using the K-S test with 95% confidence level and 10° bins, the strike distributions of the polygonal crater rims—including combined measurements from all degradational stages—show no significant difference between the two data sets (Fig. 7). Therefore, while there is a difference in the apparent polygonality of any one particular polygonal impact crater depending on the data set used, the general strike distributions of the straight rim segments of a larger population of polygonal impact craters are similar regardless of the illumination geometry. This strongly indicates that PICs are not an artifact of illumination geometry but are real geological structures that carry an important tectonic message if interpreted correctly. As can qualitatively be seen from Fig. 8, PIC data is generally congruent with information gained from ridges and graben.

DISCUSSION

Although the structural geology of the Argyre region in the light of polygonal impact craters and other structural data is not the issue of this study (in principle, this study could have been done with data from any cratered body) and will be dealt with in the companion paper, a few preliminary

qualitative remarks on the tectonics are given here. This is done in order to elucidate that there appears to be a link between the strikes of PIC rims and some sort of preferred orientations of weakness in the crust also in the Argyre region of Mars.

In the northern half of our study area (blocks A–D), an east-west strike of crater rims (craters of all degradational stages grouped together) is typical (Fig. 8). This direction is very close to (but apparently doesn't exactly match [Öhman et al. 2006]) the strike of graben in the area, as well as to Valles Marineris and the magnetic anomalies (Connerney et al. 2005). Directions both radial and concentric to the Argyre basin appear also in the data. The eastern and western rims (blocks F and G) of the basin display a prominent approximately north-south (i.e., concentric) strike of PIC rims, and an east-west strike (radial to basin) is quite prominent on the western side of the basin (block E). All these main directional patterns indicated by PIC rims mostly correlate with results obtained from other structural indicators (e.g., Thomas and Masson 1984; Schultz 1985; Scott and Tanaka 1986) (Fig. 8), indicating that polygonal impact craters in the Argyre region reflect structures of the target material very much in the same manner as the Söderfjärden crater does on Earth (Abels 2003).

The northwestern part of the study area (block A) generally has a complex rim strike pattern, probably reflecting the overlapping effects of the Tharsis rise and Argyre basin. It is noteworthy, however, that in block A the strikes of ridges and fresh crater rims generally coincide (Öhman et al. 2006; see also Öhman et al. 2005 for comparative data from Hesperia Planum). This may perhaps indicate that while in general, and especially in older terrains, the directional information seen in PICs is independent of the degradational stage of the crater, in younger terrains having a complex geotectonic history, PICs of different degradational stages (ages) may reveal different structural patterns (Table 1). This may also depend on the size of the crater and thus the depth of excavation (and therefore the type of material the crater is excavated in, irrespective of the geological surface unit). This subject is clearly worthy of further study.

Degradation cannot be the main cause of the polygonal plan view of Martian impact craters. This is clearly demonstrated by fresh, rimmed, and degraded polygonal craters all having statistically similar rim-strike distribution patterns (Fig. 5; Table 1). Of course, degradation may take advantage of preexisting weaknesses in the crust, but it probably is not creating any new major lineaments to the craters' planimetric outline (see also Eppler et al. 1983). Note that this in no way contradicts the above discussion regarding the directions of ridges and fresh PIC rims in block A: degradation itself is not important, but in complex areas the depth of excavation and the age of PICs may become important factors by indicating weaknesses that have been

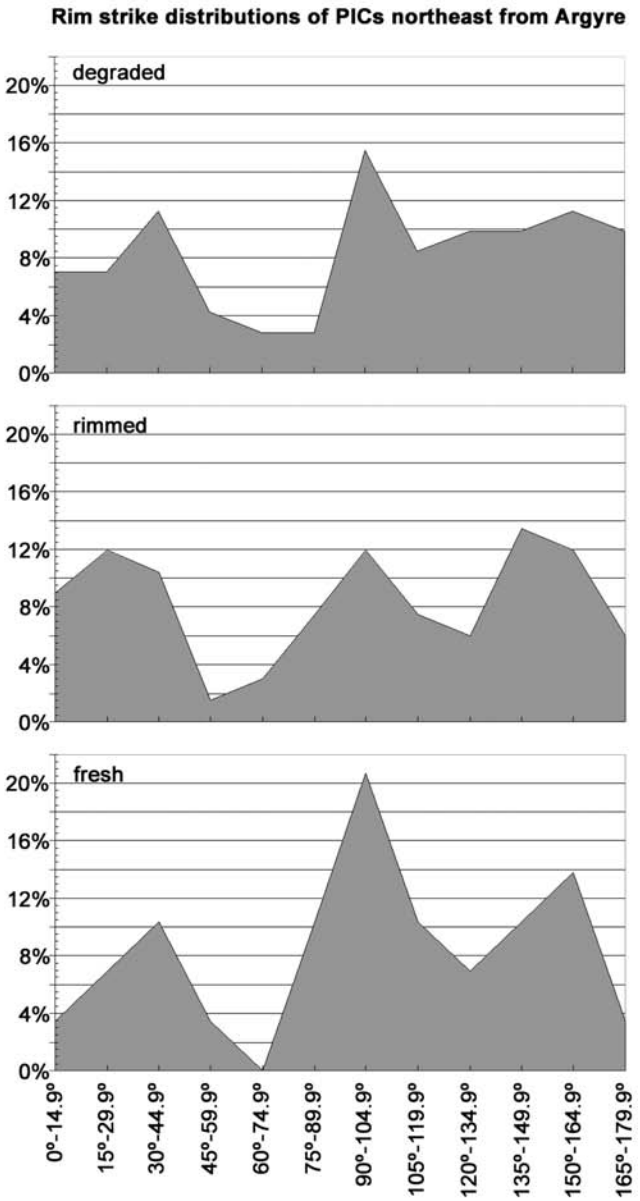

Fig. 5. Histograms of the distribution of straight rim segment strikes of degraded, rimmed, and fresh PICs from block D, northeast from the Argyre basin (Fig. 1). The total number of rim strike measurements is 71, 67, and 29 for degraded, rimmed, and fresh PICs, respectively.

dominating in different times. Unless one invokes some ad hoc theories of, e.g., recent tectonic or degradational forces deforming the shape of only some craters regardless of their age—the presently abundant circular craters have obviously not been affected by this force—the polygonal shape simply must stem from parameters affecting the cratering process itself. This result also implies that the regional fracture pattern reflected by these rim strikes has quite ancient origins, and yet remains dominant for a geologically significant time (Öhman et al., Forthcoming).

Table 1. The results of Kolmogorov-Smirnov test. Each block (center coordinates are given; blocks F and G are omitted due to low number of measurements) was tested using both 10° and 15° divisions.

Block	Division	Degraded-rimmed	Degraded-fresh	Rimmed-fresh	n_d	n_r	n_f
A	10°	×	–	+	10	55	41
34°S, 066°W	15°	×	+	+			
B	10°	+	×	+	26	60	14
34°S, 050°W	15°	+	×	+			
C	10°	+	+	+	33	86	15
34°S, 034°W	15°	+	+	+			
D	10°	+	+	+	71	67	29
34°S, 018°W	15°	+	+	+			
E	10°	+	+	+	22	107	11
50°S, 066°W	15°	+	+	+			
H	10°	+	–	×	31	25	24
50°S, 018°W	15°	+	–	+			
Total number					193	400	134

+ Samples are similar, i.e., drawn from the same population in 95% confidence level.
× Samples are practically similar, i.e., drawn from the same population in almost 95% confidence level.
– Samples are dissimilar, i.e., drawn from different populations in 95% confidence level.
The abbreviations n_d, n_r, and n_f refer to the number of rim strike measurements from degraded, rimmed, and fresh PICs, respectively.

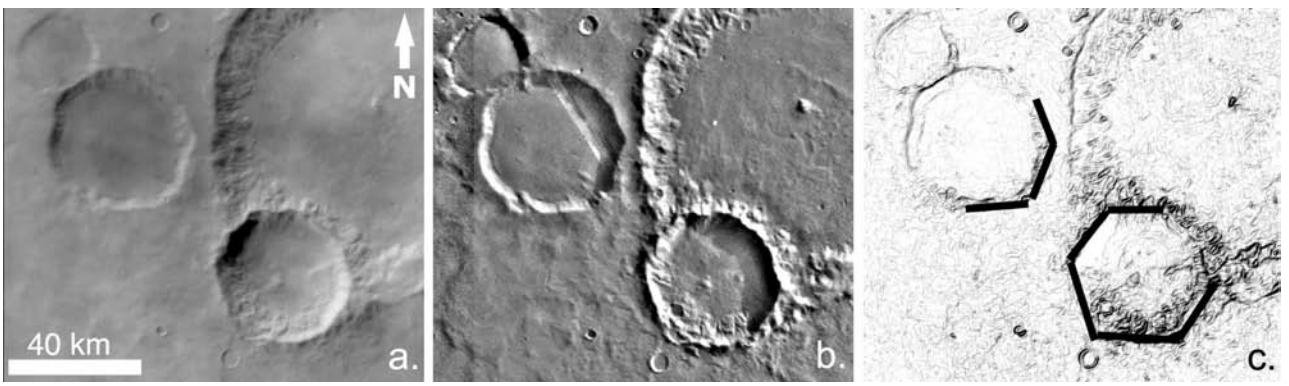

Fig. 6. Examples of polygonal craters northeast from the Argyre basin (16.4°W, 39.8°S), as seen in (a) MOC-WA images and (b) Viking images. The (c) sketch shows the straight rim segment interpretation (black lines) based on the Viking image. The same straight rim segments can be seen in both data sets, but they are much more prominent in the Viking image due to a lower incidence angle.

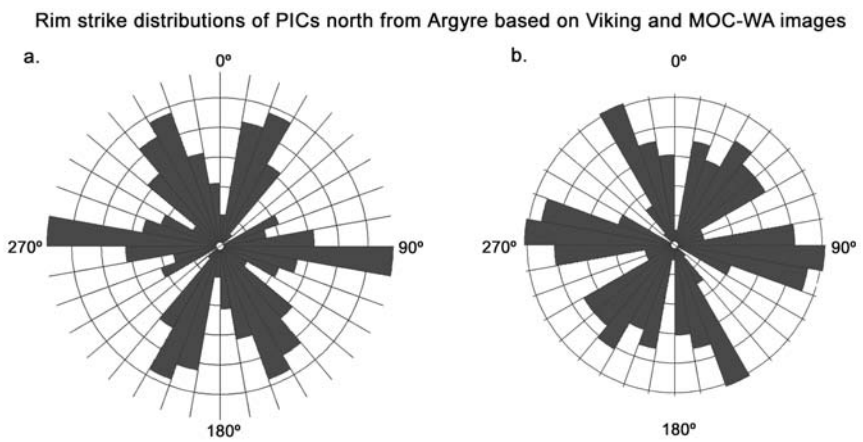

Fig. 7. Rose diagrams of the percentages of strikes of PIC straight rim segments north from the Argyre basin (26°W–58°W, 30°S–42°S; cf. Fig. 1) based on (a) a Viking MDIM 2.0 mosaic and (b) a MOC-WA mosaic. Despite some discrepancies, the overall match of the peaks and gaps is striking. The circle spacing is 2%, with the outermost circles representing 10%. The number of measurements is 94 for Viking and 98 for MOC-WA.

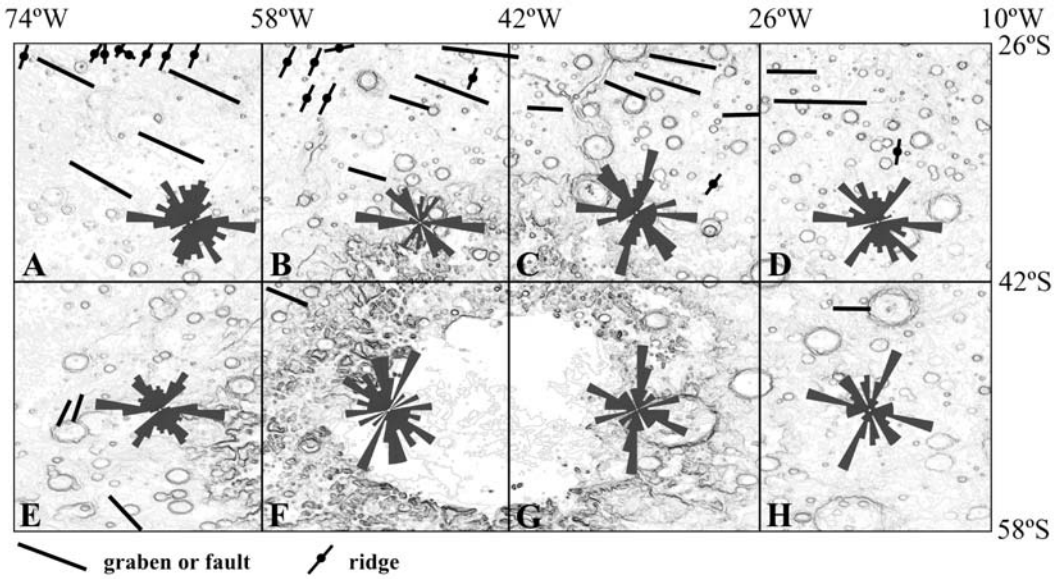

Fig. 8. A sketch of the study area with major tectonic trends as indicated by graben or faults and ridges. The rose diagrams qualitatively show the strikes of the polygonal impact craters' straight rim segments in each block (A–H). Note that data from all degradational classes is combined in the diagrams.

The polygonal shapes of craters in Fig. 2 also point toward the longevity and importance of the regional fracture pattern. The intense brecciation associated with the larger, older impact should have erased the preexisting structures of the target within the crater's rims. Despite this, the strikes of the straight rim segments of the larger crater and the smaller crater inside the larger one are almost exactly parallel. This may be explained by reactivation of the regional fractures that extend rather deep into the crust. After the formation of the larger impact crater, regional tectonic activity could have continued and deep fractures below the damage zone of the larger crater may have been reactivated. Thus, the old reactivated fractures would have affected the crust also closer to the surface, and therefore would have controlled the formation of the smaller crater—hence the almost parallel straight rim segments of the two craters.

As can be seen from Fig. 4, there are no major differences in the percentages of degradational stages between different polygonality classes, implying that the degradational stage of the craters is not reflected in their large-scale polygonality. This again strongly supports the idea that degradation is not the origin of polygonality, and coincides perfectly with the conclusion of Eppler et al. (1983), i.e., that large-scale polygonality of craters is a permanent primary feature and is not affected by later degradation processes to any major extent (see also Roddy 1978). If degradation was the cause, then one would expect to see a large amount of highly polygonal (e.g., ≥4 straight rim segments) degraded craters. Clearly, this is not the case.

In the Argyre region, we see PICs with two to six straight rim segments, with the remainder of the rim more or less following a sector of a circle. Crater shapes with a strong octagonal tendency can be seen, e.g., in the greater Hellas region (Öhman et al. 2005). Completely polygonal crater rims, however, are always very rare. This probably reflects the heterogeneity of the target material. Straight rim segments of a crater rim can most likely form only where the target has some dominating direction(s) of weakness (e.g., Fulmer and Roberts 1963; Eppler et al. 1983). Where the target is heavily fractured in different orientations, it is in essence homogenous with respect to the collapsing crater rim (or the excavation flow in the case of simple craters), thus giving rise to a roughly circular rim or a segment of a rim. The same holds when the target is very weakly fractured, e.g., in a tectonically very stable area, or when the target material's properties are not susceptible to fracturing (loose or only moderately compacted sediments, etc.). The spacing of fractures with respect to the crater diameter probably also plays a role, especially in the case of small craters, as was shown by Fulmer and Roberts (1963): if the spacing of the dominating fractures is large compared to the crater diameter, the crater of course cannot "know" the fractures and thus its shape cannot reveal anything about them.

The illumination geometry of the data set used does affect the apparent polygonality of any individual impact crater (Schultz 1976) (Fig. 6). However, we are confident that the rim strikes we are measuring are statistically and geologically meaningful and real. This is illustrated by the statistical match in the comparison between strike distributions of PICs apparent in both Viking and MOC-WA images (Fig. 7).

The rim of an impact crater does indeed seem to have a "memory" of the preexisting structures of the target material, as has been shown by, e.g., Shoemaker (1963) and Roddy

(1978) regarding the Barringer crater, by Schultz (1976) regarding lunar craters, and by our work with craters in the Hellas (Öhman et al. 2005) and the Argyre regions on Mars (this study; Öhman et al. 2006). This has also been supported by experimental studies (Fulmer and Roberts 1963; Gault et al. 1968). We have in this study ruled out degradation and illumination geometry as significant factors in the PIC rim strikes (see also a brief note in Binder and McCarthy 1972). Thus, it is justifiable to state that with a reasonable amount of measurements, polygonal crater data can be successfully used in the regional scale interpretation of the structural patterns on a cratered surface.

Our study also indicates that while acoustic fluidization (e.g., Melosh 1979; Melosh 1989; Melosh and Ivanov 1999) or some other mechanism (e.g., O'Keefe and Ahrens 1993) probably "lubricates" the zone beneath the apparent crater, some of the near-surface rocks of the crater rim must behave in a brittle way during the modification stage, or otherwise the collapsing rim wouldn't reflect the structure of the target in a way exemplified by polygonal craters. Thus, our results corroborate the conclusions about rim behavior based on observations of lunar craters' rim terraces (Melosh 1989).

CONCLUSIONS

Based on polygonal impact crater data from the Argyre region, which is largely confirmed by statistical analysis, the following conclusions can be drawn:

- The dominating regional fracture directions of target material indicated by polygonal impact craters are independent of the degradational stage of the crater.
- Degradation of craters does not create large-scale polygonality in the planimetric shape of the crater rim. Instead, polygonality originates from target structures and the cratering process itself.
- On a regional scale, illumination geometry of the data set used does not affect the interpretations of dominating fracture directions.
- In general, polygonal impact craters reveal structural patterns similar to other indicators of tectonism, e.g., graben and ridges. Further studies on the subject are nevertheless in order.
- The near-surface rocks of the apparent crater rim behave in a brittle manner during the crater modification stage.
- Based on previous works and our conclusions, polygonal impact craters are obviously a useful and a reliable tool in mapping regional structural patterns on cratered surfaces.

Acknowledgments–We gratefully acknowledge the thoughtful reviews by Prof. Boris Ivanov and Dr. Jens Ormö, as well as the valuable comments made by Associate Editor Dr. Alex Deutsch, which significantly improved the contents and structure of the manuscript. Phil. Lic. Terhi Törmänen's assistance with projection conversions is acknowledged with great gratitude. M.Sc. Jarmo Korteniemi is thanked for his help with MOLA data. Thanks are also due to M.Sc. Jari Päkkilä from the Department of Mathematical Sciences, University of Oulu, for his comments on the statistical aspects of this work.

The authors acknowledge the use of Viking imagery and Mars Orbiter Laser Altimeter data obtained from NASA's Planetary Data System, the Mars Orbiter Camera images processed by Malin Space Science Systems, as well as the efforts of the respective science teams. This research has also made use of data provided by NASA's Nordic Regional Planetary Image Facility in the University of Oulu and NASA's Astrophysics Data System Bibliographic Services. The Vilho, Yrjö and Kalle Väisälä Foundation of the Finnish Academy of Science and Letters, the Finnish Graduate School in Geology, and the Magnus Ehrnrooth Foundation are thanked for partial financial support.

Editorial Handling—Dr. Alexander Deutsch

REFERENCES

Abels A. 2003. Investigation of impact structures in Finland (Söderfjärden, Lumparn, Lappajärvi) by digital integration of multidisciplinary geodata. Ph.D. thesis, FB Geowissenschaften, Westfälische Wilhelms-Universität, Münster, Germany.

Acuña M. H., Connerney J. E. P., Ness N. F., Lin R. P., Mitchell D., Carlson C. W., McFadden J., Anderson K. A., Rème H., Mazelle C., Vignes D., Wasilewski P., and Cloutier P. 1999. Global distribution of crustal magnetization discovered by the Mars Global Surveyor MAG/ER experiment. *Science* 284:790–793.

Baldwin R. B. 1963. *The measure of the Moon.* Chicago: The University of Chicago Press. 488 p.

Barlow N. G., Boyce J. M., Costard F. M., Craddock R. A., Garvin J. B., Sakimoto S. E. H., Kuzmin R. O., Roddy D. J., and Soderblom L. A. 2000. Standardizing the nomenclature of Martian impact crater ejecta morphologies. *Journal of Geophysical Research* 105:26,733–26,738.

Binder A. B. and McCarthy D. W., Jr. 1972. Mars: The lineament systems. *Science* 176:279–281.

Cheeney R. F. 1983. *Statistical methods in geology.* London: George Allen & Unwin. 169 p.

Chicarro A. F., Schultz P. H., and Masson P. 1985. Global and regional ridge patterns on Mars. *Icarus* 63:153–174.

Connerney J. E. P., Acuña M. H., Wasilewski P. J., Ness N. F., Rème H., Mazelle C., Vignes D., Lin R. P., Mitchell D. L., and Cloutier P. A. 1999. Magnetic lineations in the ancient crust of Mars. *Science* 284:794–798.

Connerney J. E. P., Acuña M. H., Ness N. F., Kletetschka G., Mitchell D. L., Lin R. P., and Reme H. 2005. Tectonic implications of Mars crustal magnetism. *Proceedings of the National Academy of Sciences,* doi:10.1073/pnas.0507469102.

Davis J. C. 2002. *Statistics and data analysis in geology,* 3rd ed. New York: John Wiley & Sons. 638 p.

Eppler D. T., Ehrlich R., Nummedal D., and Schultz P. H. 1983. Sources of shape variation in lunar impact craters: Fourier shape analysis. *Geological Society of America Bulletin* 94:274–291.

Fulmer C. V. and Roberts W. A. 1963. Rock induration and crater shape. *Icarus* 2:452–465.

Garvin J. B., Sakimoto S. E. H., and Frawley J. J. 2003. Craters on Mars: Global geometric properties from gridded MOLA topography (abstract #3277). The Sixth International Conference on Mars. CD-ROM.

Gault D. E., Quaide W. L., and Oberbeck V. R. 1968. Impact cratering mechanics and structures. In *Shock metamorphism of natural materials,* edited by French B. M. and Short N. M. Baltimore: Mono Book Corporation. pp. 87–99.

Grant J. A. and Schultz P. H. 1993. Degradation of selected terrestrial and Martian impact craters. *Journal of Geophysical Research* 98: 11,025–11,042.

Hiesinger H. and Head J. W. III. 2002. Topography and morphology of the Argyre basin, Mars: Implications for its geologic and hydrologic history. *Planetary and Space Science* 50:939–981.

Hodges C. A. 1980. Geologic map of the Argyre quadrangle of Mars. U.S. Geological Survey Map #I-1181 (MC-26).

Kirk R. L., Lee E. M., Sucharski R. M., Richie J., Grecu A., and Castro S. K. 2000. MDIM 2.0: A revised global digital image mosaic of Mars (abstract #2011). 31st Lunar and Planetary Science Conference. CD-ROM.

Kopal Z. 1966. *An introduction to the study of the Moon.* Dordrecht, The Netherlands: D. Reidel Publishing Company. 466 p.

Laurén L., Lehtovaara J., Boström R., and Tynni R. 1978. On the geology and the Cambrian sediments of the circular depression at Söderfjärden, western Finland. *Geological Survey of Finland Bulletin* 297:1–81.

Melosh H. J. 1979. Acoustic fluidization: A new geologic process? *Journal of Geophysical Research* 84:7513–7520.

Melosh H. J. 1989. *Impact cratering: A geologic process.* New York: Oxford University Press. 245 p.

Melosh H. J. and Ivanov B. 1999. Impact crater collapse. *Annual Review of Earth and Planetary Sciences* 27:385–415.

Neumann G. A., Zuber M. T., Wieczorek M. A., McGovern P. J., Lemoine F. G., and Smith D. E. 2004. Crustal structure of Mars from gravity and topography. *Journal of Geophysical Research*, doi:10.1029/2004JE002262.

Öhman T., Aittola M., Kostama V.-P., and Raitala J. 2005. The preliminary analysis of polygonal impact craters within greater Hellas region, Mars. In *Impact tectonics,* edited by Koeberl C. and Henkel H. Berlin Heidelberg: Springer-Verlag. pp. 131–160.

Öhman T., Aittola M., Kostama V.-P., and Raitala J. 2006. Preliminary geological analysis of polygonal impact crater data from Argyre region, Mars (abstract #1236). 37th Lunar and Planetary Science Conference. CD-ROM.

Öhman T., Aittola M., Kostama V.-P., and Raitala J. Forthcoming. The geologic implications of polygonal impact craters within Argyre region, Mars. *Meteoritics & Planetary Science*.

O'Keefe J. D. and Ahrens T. J. 1993. Planetary cratering mechanics. *Journal of Geophysical Research* 98:17,011–17,028.

Pike R. 1980. Control of crater morphology by gravity and target type: Mars, Earth, Moon. Proceedings, 11th Lunar and Planetary Science Conference. pp. 2159–2189.

Purucker M., Ravat D., Frey H., Voorhies C., Sabaka T., and Acuña M. 2000. An altitude-normalized magnetic map of Mars and its interpretation. *Geophysical Research Letters* 27:2449–2452.

Raitala J. 1985. The bedrock of the Vaasa circular structure, western Finland. *Earth, Moon, and Planets* 33:133–155.

Roddy D. J. 1978. Pre-impact geologic conditions, physical properties, energy calculations, meteorite and initial crater dimensions and orientations of joints, faults and walls at Meteor Crater, Arizona. Proceedings, 9th Lunar and Planetary Science Conference. pp. 3891–3930.

Rossi A. P., Baliva A., and Piluso E. 2003. New evidences of an impact origin for Temimichat crater, Mauritania (abstract #1882). 34th Lunar and Planetary Science Conference. CD-ROM.

Schultz P. 1976. *Moon morphology.* Austin, Texas: University of Texas Press. 626 p.

Schultz R. A. 1985. Assessment of global and regional tectonic models for faulting in the ancient terrains of Mars. *Journal of Geophysical Research* 90:7849–7860.

Schultz P. H., Schultz R. A., and Rogers J. 1982. The structure and evolution of ancient impact basins on Mars. *Journal of Geophysical Research* 87:9803–9820

Scott D. H. and Tanaka K. L. 1986. Geologic map of the western equatorial region of Mars. U.S. Geological Survey Map #I-1802-A.

Shoemaker E. M. 1963. Impact mechanics at Meteor Crater, Arizona. In *The Moon, meteorites and comets,* edited by Middlehurst B. M. and Kuiper G. P. Chicago: The University of Chicago Press. pp. 301–336.

Talvitie J., Pernu T., and Raitala J. 1975. The circular Vaasa structure in the Baltic Shield, western Finland. Department of Geophysics, University of Oulu, Contribution #59. 15 p.

Tanaka K. L., Scott D. H., and Greeley R. 1992. Global stratigraphy. In *Mars,* edited by Kieffer H. H., Jakosky B. M., Snyder C. M., and Matthews M. S. Tucson, Arizona: The University of Arizona Press. pp. 345–382.

Thomas P. G. and Masson P. H. 1984. Geology and tectonics of the Argyre area on Mars: Comparisons with other basins in the solar system. *Earth, Moon, and Planets* 31:25–42.

Wichman R. W. and Schultz P. H. 1989. Sequence and mechanisms of deformation around the Hellas and Isidis impact basins on Mars. *Journal of Geophysical Research* 94:17,333–17,357.